Electron glass signatures up to room temperature in disordered insulators

Julien Delahaye, T Grenet

Electron glass signatures up to room temperature in disordered insulators

J. Delahaye and T. Grenet

Univ. Grenoble Alpes, CNRS, Institut Néel, 38000 Grenoble, France

E-mail: julien.delahaye@neel.cnrs.fr

November 2021

Abstract. This paper describes the observation of non-equilibrium field effects at room temperature in four disordered insulating systems: granular Al, discontinuous Au, amorphous NbSi and amorphous InOx thin films. The use of wide enough gate voltage ranges and a cautious analysis of the data allow us to uncover memory dips, the advocated hallmark of the electron glass, in the four systems. These memory dips are found to relax slowly over days of measurements under gate voltage changes, reflecting the impossibility for the systems to reach an equilibrium state within experimentally accessible times. Our findings demonstrate that these electrical glassy effects, so far essentially reported at cryogenic temperatures, actually extend up to room temperature.

1. Introduction

As electrons are very light particles, they are generally associated with very short characteristic times in solids. The fact that slow and glassy phenomena are found in the electronic properties of some disordered insulating systems is thus a challenging and fascinating issue (see [1] for a review). These glassy phenomena are characterized by two main features. First, the electrical conductance is found to decrease slowly after a rapid cooling. This decrease, logarithmic in time, continues at least over weeks of measurements and reflects the impossibility for the system to reach a true equilibrium state. Second, when the disordered insulating systems are thin films used as the (weakly) conducting channel of MOSFET devices, a fast gate voltage (V_g) sweep, performed after a long enough time has been spent under a fixed V_g (subsequently noted V_{geq}), reveals a conductance minimum centred on this V_g value. This field effect feature, called the "memory dip" (MD), is the fingerprint of the gate voltage history experienced by the sample. This MD behaviour and other related features, first investigated in detail in amorphous and microcrystalline indium oxide (InOx) films [2, 3], have since then proven to be rather common among disordered insulating systems. Indeed, they were also observed in discontinuous and ultrathin continuous films of metals [4, 5, 6], in granular Al [7, 8], in oxidized Be [9], in microcrystalline Tl_2O_{3-x} [10], in amorphous

and microcrystalline metal-semiconductor alloys (NbSi [11, 12], GeSbTe [13], GeTe [14], GeBiTe [15]), with the notable exception of standard doped semi-conductors. It was soon suggested that these glassy features are the signature of the electron glass [1]. This glassy state, theoretically predicted in the 80ies, stems from the coexistence of disorder and ill screened electron-electron interactions in disordered systems [16, 17, 18]. Recently it was found that the upper bound of the relaxation time distribution decreases and becomes measurable when both the charge carrier concentration and resistance per square are diminished in amorphous InOx films [19], strongly supporting the electron glass hypothesis.

Interestingly, most of the experimental works devoted to these glassy effects have been limited so far to the liquid helium temperature (T) range. At 4 K, MDs represent typically a few % of the conductance when the sheet resistance R_{s4K} lies in the range $1\ M\Omega - 1\ G\Omega$. In the few studies where higher T were explored (up to about 50 K), the relative amplitudes of the MDs were found to decrease strongly when T increases (as a power law in granular Al films [8], exponentially in InOx films [20]). In InOx films, such a decrease led to the conclusion that glassy effects are indeed absent or too small to be measurable above a few tens of kelvins [21]. But two experimental findings have recently called the generality of this conclusion into question. First, MDs of the order of 1 % were reported at room T in insulating discontinuous Au films [22, 23]. Second, although very small (less than 0.02 %), traces of MDs were found to persist up to room T in an amorphous NbSi thin film [11].

Whether room T glassy effects are exceptional or widespread is the question we would like to answer in this paper. In a first part, we present field effect measurements performed at room T on insulating granular Al films covering a large resistance range. MDs that respond slowly to V_{geq} changes are observed in all the films studied. Their amplitudes can be as large as a few percent if the resistance of the film is high enough. These results are compared to those obtained on discontinuous Au and on amorphous NbSi. We then demonstrate that MDs are also present in InOx films at room T, although they are mixed with another conductance relaxation of different nature. We end by discussing why room T glassy effects have been so scarce in previous studies, and what are the new perspectives offered by our findings.

2. Samples and measurement set-up

The granular Al films measured in this study are 10 nm-thick. They were made by the electron beam deposition of pure Al in a partial pressure of O_2 [8]. The Al evaporation rate was 1.8 $\AA/s$ and a large range of room T sheet resistances was obtained by changing the O_2 partial pressure, from $R_{s300K} \simeq 100\ k\Omega$ ($P_{O2} = 2.4 \times 10^{-5}\ mbar$) up to 100 $G\Omega$ ($P_{O2} = 3.4 \times 10^{-5}\ mbar$).

The amorphous NbSi film is 2.5 nm thick and has a Nb content of 13 %. This sample, already measured at 4.2 K in previous works [11, 12] was made by the co-deposition of Nb and Si at room T under high vacuum (typically a few $10^{-8}\ mbar$) [24].

Its sheet resistance at room T is 25 $k\Omega$ (100 $M\Omega$ at 4.2 K).

The insulating discontinuous Au films were made by the electron beam deposition of Au at room T. The evaporation rate was varied between 0.2 and 2 $\mathring{A}/s$, under a residual vacuum of 10^{-6} to 10^{-7} mbar. The films have nominal thicknesses of 6 - 7 nm and their SEM pictures reveal a characteristic maze structure (see Fig. 1). Their resistance was found to increase after deposition, as is commonly observed in insulating discontinuous Au films [25], and becomes roughly stable after a few days of measurements. The films used in this study have relaxed R_{s300K} values between 30 $M\Omega$ and 30 $G\Omega$. 20 nm-thick gold contacts were evaporated prior to the discontinuous Au film.

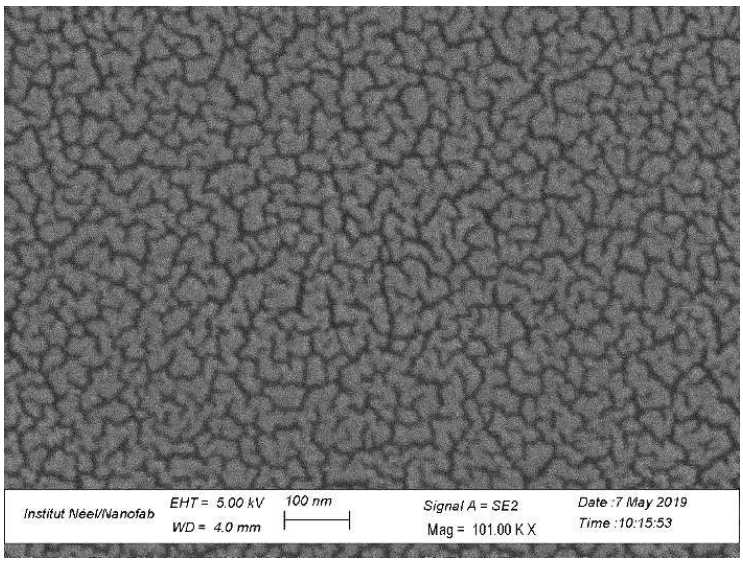

Figure 1. SEM picture of a discontinuous Au film evaporated at room T on a Si_{++}/SiO_2 substrate. Nominal thickness: 7.0 nm; $R_{s300K} = 300$ $M\Omega$.

We also show results obtained on a 10 nm-thick amorphous InOx film made by the electron beam deposition of In_2O_3 at a rate of 1 $\mathring{A}/s$, under a partial O_2 pressure of 2×10^{-4} $mbar$, having $R_{s300K} \simeq 300$ $k\Omega$.

In order to perform field effect measurements, the disordered insulating thin films were all deposited on highly doped Si wafers (Si_{++}, the gate) coated with 100 nm of thermally grown SiO_2 (the gate insulator). The active channel has a typical size of 1 $mm \times 1$ mm and its electrical conductance G was measured by using a two-terminal DC technique. For room T measurements (T between 293 - 296 K), a bias voltage of about 1 V was applied with a low noise voltage source, and the current was measured with the Femto DLPCA 200 current amplifier. Unless otherwise mentioned, the device charging currents induced by V_g changes were negligible compared to the bias current variations related to the slow processes discussed in this paper (this was checked by performing V_g sweeps with zero bias, which allow the measurement of charging currents alone). V_g could be varied between -30 V and 30 V, far enough from the practical breakdown limit of our 100 nm-thick SiO_2 insulating barrier which is around 50 V.

No significant leaking current was detected within this V_g range. All the samples were mounted in a metallic enclosure and maintained in vacuum during the measurement campaigns.

3. Evidence for room temperature memory dips in granular Al films

We first sought to find out whether electron glass features are present at room T in granular Al films. At 4 K, their hallmark is the existence of a MD centred on the cool-down V_g [26] and the slow formation of a new one if V_g is set to a new value [7, 8]. At room T, we first simply examined whether a MD exists centred on $V_g = V_{geq}$ applied for long enough. The protocol is thus the following: V_g is fixed to 0 V for a long enough time (one day or more) before fast V_g sweeps are performed around this value. The V_g sweeps between -30 V and 30 V are typically 200 s long and can be repeated every 2000 - 4000 s in order to average and reduce the noise level of the curves (these parameters can differ by a factor of 2 depending on the sample). The results (black curves) are displayed in Fig. 2 for four different films having R_{s300K} values between 46 $k\Omega$ and 91 $G\Omega$. The less resistive film with $R_{s300K} = 46$ $k\Omega$ has a 4.2 K resistance of 8 $M\Omega$, typical of the samples usually measured in liquid He.

The $G(V_g)$, even when corrected for transitory charging effects (significant only when R_s is above 1 $G\Omega$), reveal either no conductance minimum (samples with $R_{s300K} = 46$ $k\Omega$ and 1 $M\Omega$) or a minimum which is not centred on V_{geq} (samples with $R_{s300K} = 365$ $M\Omega$ and 91 $G\Omega$). However, as we shall demonstrate below, MDs are indeed present in all the samples, although they do not show here under their usual 4 K form. First, they coexist with a comparatively large "normal" linear field effect which gives rise to a monotonic increase of the conductance with V_g. This linear field effect contribution is usually attributed to the energy dependence of the thermodynamic density-of-states at the Fermi level [21]. Second, the MDs extend over a V_g range larger than our accessible V_g window (-30 V to 30 V) and only the bottom of the dips is visible.

If we subtract a linear contribution from each $G(V_g)$ curves so as to equalize the conductance at -20 V and 20 V, we get conductance minima (red curves in Fig. 1) that are roughly symmetrical around $V_{geq} = 0$ V. The conductance change between $V_{geq} = 0$ V and V_g can thus be decomposed in two parts : a linear one, ΔG_{lin}, deduced from the V_g slope of the linear contribution, and a (roughly) symmetrical one, $\Delta G = G(V_g) - G(V_{geq} = 0\ V) - \Delta G_{lin}(V_g)$. The relative amplitudes $\Delta G_{lin}/G$ and $\Delta G/G$ of respectively the linear and symmetrical contributions measured between 0 V and 30 V both decrease as R_s is lowered (see Fig. 3). They are roughly the same as long as $R_s > 1$ $G\Omega$, but, below this resistance range, the symmetrical component decreases faster than the linear one, which explains why no conductance minima is discernable in low R_s films.

In order to prove that these conductance minima are MDs, we still need to verify that they evolve after a V_{geq} change. This is shown in Fig. 4 where $G(V_g)$ curves have been measured at different times after V_{geq} was changed from 0 V to 20 V. The $V_{geq} = 0$ V

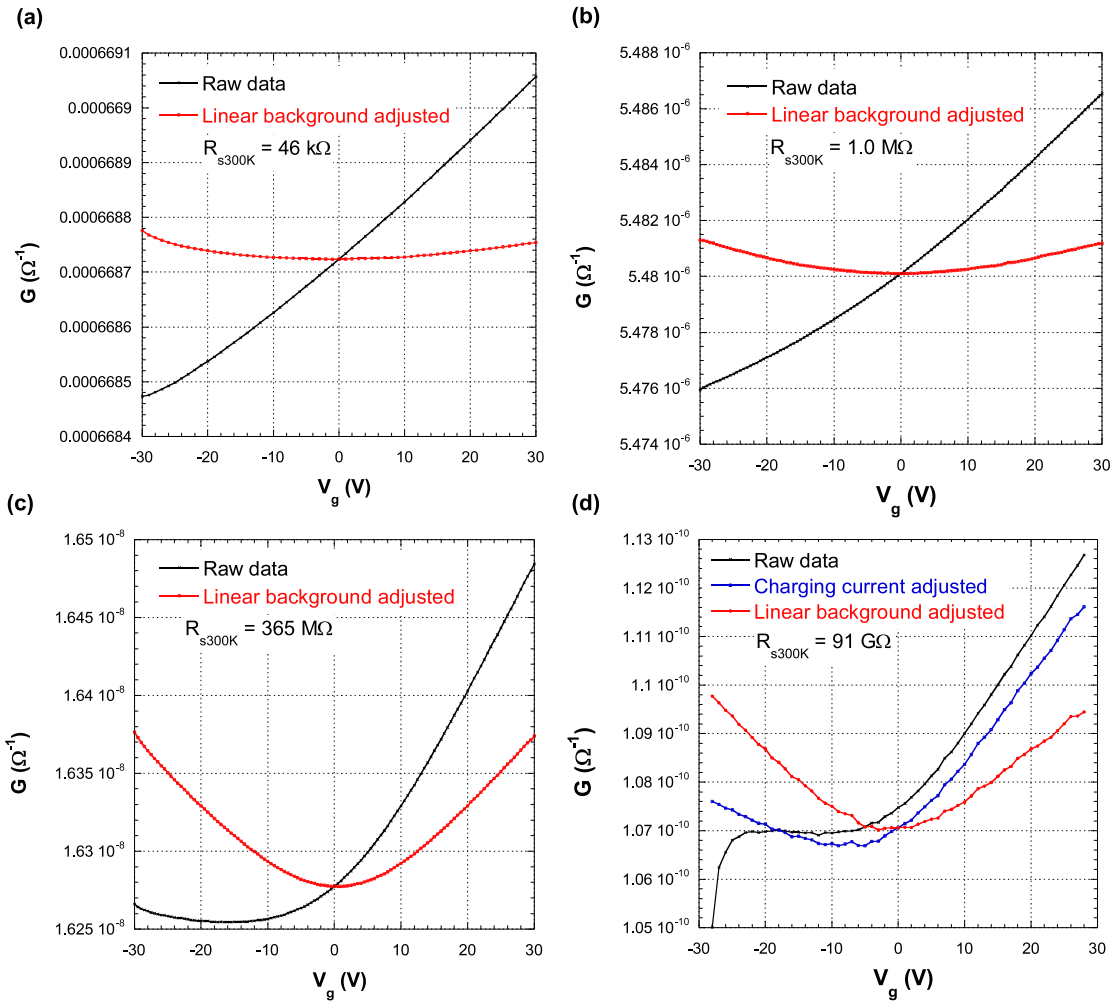

Figure 2. $G(V_g)$ curves measured at room T after about one day under $V_{geq} = 0\ V$ in four different granular Al films. Black symbols: raw data; blue symbols: charging current adjusted data (this correction is necessary only when $R \geq 1\ G\Omega$); red symbols: linear background adjusted data (refer to text for details). (a) $R_{s300K} = 46\ k\Omega$; (b) $R_{s300K} = 1.0\ M\Omega$; (c) $R_{s300K} = 365\ M\Omega$; (d) $R_{s300K} = 91\ G\Omega$.

linear background correction is assumed to remain the same in a given sample when V_{geq} is changed. The conductance minimum, first centred on 0 V, clearly moves toward the new V_{geq} value. The fact that it is not centred on the new V_{geq} value for short times can simply be explained by the strong overlap between the new and the old dips (see the discussion below).

We now discuss the MD widths. For comparison, the less resistive film of our series ($R_{s300K} = 46\ k\Omega$) was measured at 4.2 K on the same V_g range (left panel of Fig. 5). At 4.2 K, the full MD is clearly visible and much thinner than our V_g window, with a full width at half maximum (FWHM) of about only 1.5 V, in agreement with previous studies [27]. The T evolution of the MD shape was studied previously between 4 K and 20 K in granular Al films [8]. It was found that, except at the lowest T, the MDs

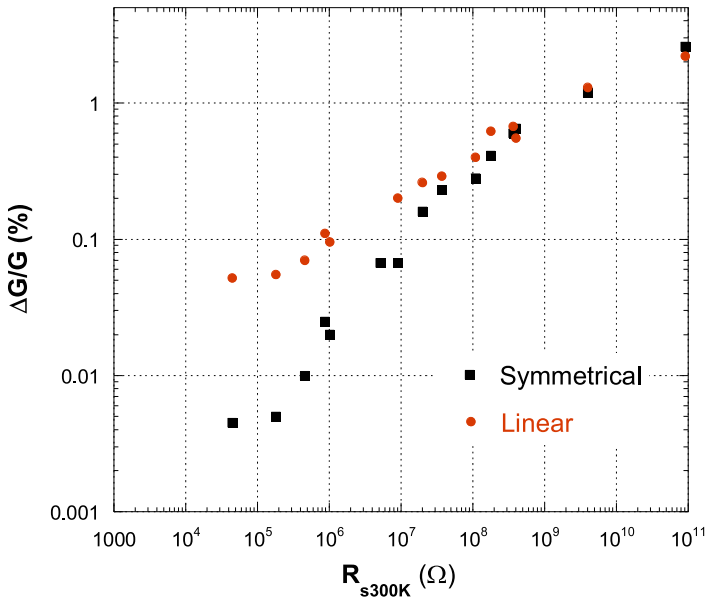

Figure 3. Evolution of the symmetrical (black square symbols) and linear (red dot symbols) field effect components with R_{s300K} in different granular Al films. Their relative amplitudes were calculated from $G(V_g)$ curves between 0 V and 30 V (see the text for details).

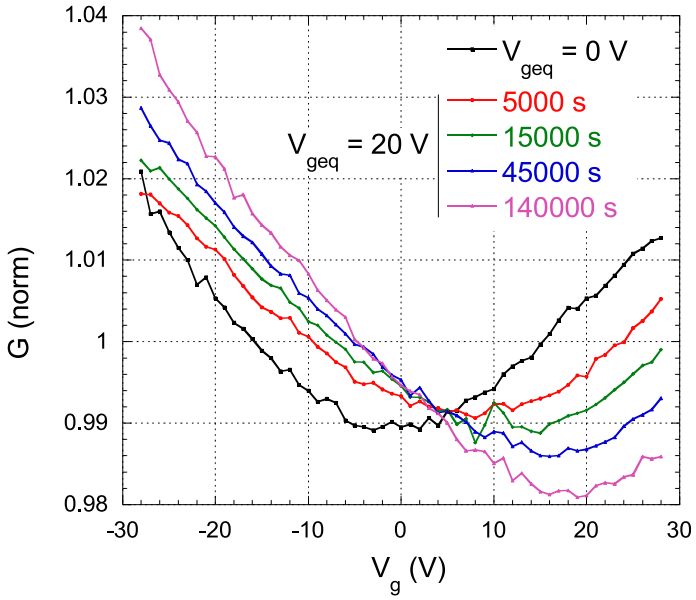

Figure 4. Normalized $G(V_g)$ curves measured at room T before (black curve) and at different times after V_{geq} was changed from 0 V to 20 V (the same linear background has been subtracted from all the raw curves). The sample, a granular Al film with $R_{s300K} = 91\ G\Omega$, was first kept for a few days under $V_{geq} = 0\ V$.

are well described by a Lorentzian shape and that their typical widths grow roughly

linearly with T. Assuming that this law remains valid up to room T and that the 4.2 K width is roughly R_s independent [27], we expect a width of about 100 V at 300 K. By fitting the red curves of Fig. 2 with Lorentzian functions centred on 0 V (the equilibrium V_g), we get FWHM estimates of 150 V, 120 V, 90 V and 70 V for granular Al films of respectively $R_s = 46\ k\Omega$, 1.0 $M\Omega$, 365 $M\Omega$ and 91 $G\Omega$, in rough agreement with our expectation. We observed a similar decrease in the FWHM values as R_s increases at 4 K but with no explanation so far. Such a fit (red line) and the measured $G(V_g)$ curve (black symbols) are plotted in the right panel of Fig. 5 for the $R_{s300K} = 1.0\ M\Omega$ film. It thus appears clearly that for all films, our V_g window of 60 V allows us to only measure the bottom of the MD, most of it being outside this V_g range. Such a result stresses an important practical point: in order to be able to measure room T glassy effects in granular Al films, the V_g range investigated should be large enough. We shall see below that this conclusion applies to other systems as well.

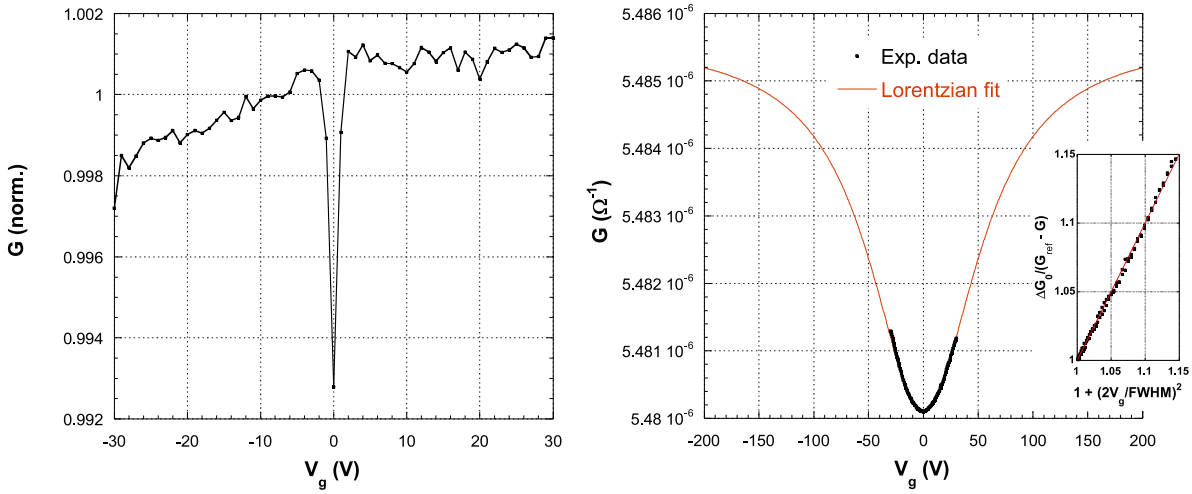

Figure 5. Left panel: normalized $G(V_g)$ curves measured 16800 s after a cooling from room T to 4.2 K in a granular Al film ($R_{s300K} = 46\ k\Omega$, $R_{s4.2K} = 8.0\ M\Omega$). Right panel: $G(V_g)$ curve measured at room T (black symbols) and its Lorentzian fit $G = G_{ref} - \Delta G_0/(1 + (2V_g/FWHM)^2)$ (red line, $G_{ref} = 5.5 \times 10^{-6}\ \Omega^{-1}$, $\Delta G_0 = 5.5 \times 10^{-9}\ \Omega^{-1}$, $FWHM = 120\ V$) in a granular Al film having $R_{s300K} = 1.0\ M\Omega$. Insert: $\Delta G_0/(G_{ref} - G)$ as a function of $1 + (2V_g/FWHM)^2$ between -20 V and 20 V. The uncertainty about the FWHM value is of $\pm 20\ V$.

The relative amplitudes of the MDs are given by the symmetrical component values $\Delta G/G$, when $|V_g - V_{geq}|$ is large enough so that ΔG saturates. We can get lower bound values by comparing the conductance at $V_g = V_{geq} = 0\ V$ and at $V_g = 30\ V$ after one day or more under V_{geq}, that is by measuring $\Delta G(30V)/G$. A clear increase of $\Delta G(30V)/G$ is observed with R_s, as seen in previous 4.2 K studies [27]: this lower bound value reaches 2.5 % when $R_{s300K} \sim 100\ G\Omega$, and is still measurable although very small (4.5×10^{-3} %) when $R_{s300K} \sim 100\ k\Omega$ (blue symbols in Fig. 6). According to our Lorentzian fits, the actual values of the full MDs ($\Delta G_0/G$) are 2.5 and 4 times

larger for R_s around respectively 100 $G\Omega$ and 100 $k\Omega$. These relative MD amplitudes are only a few times smaller than the ones measured at 4.2 K on granular Al films having similar R_s values (see Fig. 6). Note that since the MD amplitudes are believed to depend only logarithmically on the sweep parameters and the time spent under V_{geq} (see the dynamics tests below), the comparison between the different samples highlighted in Fig. 6 is meaningful although these parameters were not strictly the same for the different samples.

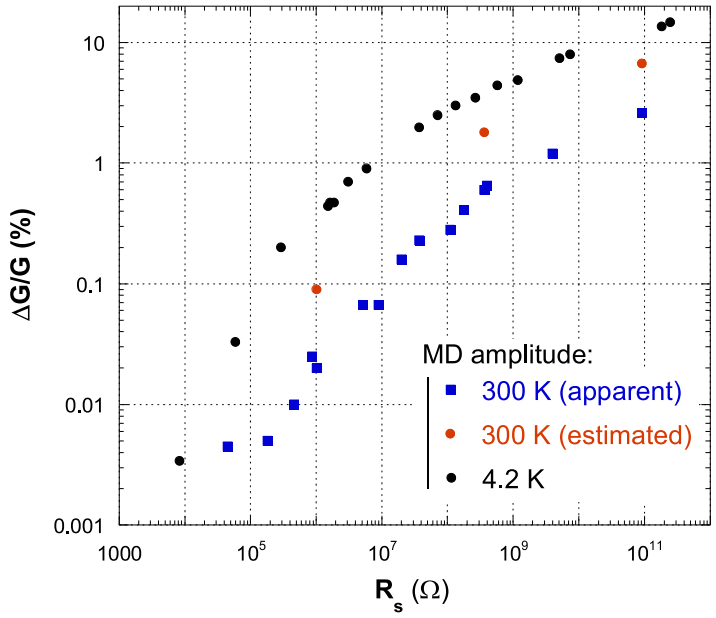

Figure 6. MD amplitude as a function of R_s in granular Al films. Black symbols: 4.2 K values as a function of R_{s4K} (the full MDs are visible at this temperature, data from Ref. [27]). Red and blue symbols : room T values as a function of R_{s300K}. Red symbols: the room T amplitudes of the MD are estimated from Lorentzian fits of the data between -30 V and 30 V (ΔG is given by the parameter ΔG_0 of the Lorentzian fit). Blue symbols: the room T amplitudes are measured between 0 V and 30 V ($\Delta G = \Delta G(30\ V)$).

To further characterize the conductance dynamics associated with V_{geq} changes, we applied the isothermal 2 dips protocol, usually used at 4 K [28, 21, 8]: after a long stay of one day or more under $V_{geq1} = 0\ V$, V_{geq} is set to a new value $V_{geq2} = 20\ V$ for a given time t_w (step 1), and then shifted back to V_{geq1} (step 2). The time evolution of the conductance at -20 V (ref. value), 0 V and 20 V are recorded during step 1 and step 2. Typical results for the less resistive granular Al sample (hence the high noise level of the curves) are plotted in Fig. 7. The difference between the conductance value at -20 V (ref.) and at 20 V (V_{geq2}) increases as a logarithm of the time elapsed during step 1 (new MD formation), and follows the erasure function $A\ln(1+t_w/t)$ during step 2 (new MD erasure), as is commonly observed at 4.2 K in granular Al and InOx films [8, 29]. This shows that also at room T, the conductance relaxations are associated to log-uniformly distributed relaxation times, at least in the time window explored here

($\sim$ 100 s to 10^5 s), with modes effectively relaxing back and forth under V_{geq} changes. Similar logarithmic relaxations are observed at room T in all our granular Al films.

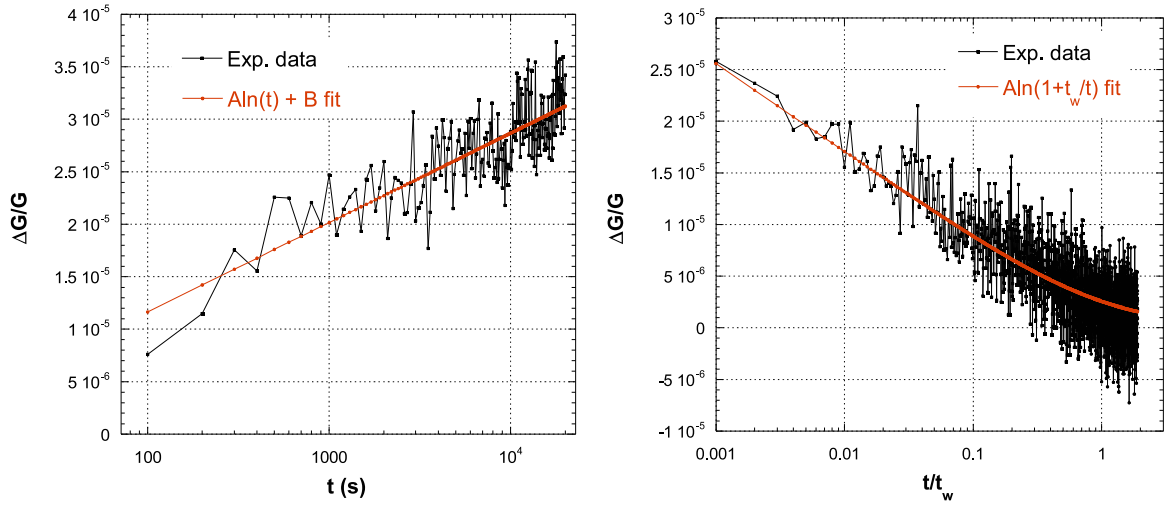

Figure 7. Left panel: time evolution of $\Delta G/G = [G(-20\ V) - G(20\ V)]/G(-20\ V)$ reflecting the growth of the new MD at 20 V after V_{geq} was changed from 0 to 20 V. Right panel: erasure of the same 20 V MD (formed during $t_w = 20000\ s$) after V_{geq} is switched back to 0 V. The linear field effect contribution was removed to show the MD amplitude going asymptotically to zero in the right panel. Granular Al film, $R_{s300K} = 46\ k\Omega$.

4. Comparison with amorphous NbSi and discontinuous Au films

We will now see how granular Al compares with the two other systems in which room T glassy effects have been previously reported, i.e. amorphous NbSi and discontinuous Au films. In the amorphous NbSi film measured in Refs. [11, 12] ($R_{s300K} = 25\ k\Omega$), a symmetrical conductance minimum centred on the equilibrium gate voltage value is visible at room T after the subtraction of a linear field effect contribution (left panel of Fig. 8). This conductance minimum moves slowly after a V_{geq} change (right panel of Fig. 8) and is therefore a MD. Its amplitude between 0 V and 30 V is of 0.015 %, slightly higher than what is found in granular Al films of similar R_s values. Like in granular Al films, only the bottom of the MD is visible in our V_g window: a fit with a Lorentzian shape gives a full width at half maximum of 140 V ($\pm 20\ V$) and a full amplitude of 0.09 %. MD drifts are observed over days after V_{geq} changes, which is a clear indication that very long relaxation times are still involved in the room T dynamics.

In discontinuous Au films made at room T, MDs are present but with some specificities. First, the linear field effect has a negative slope, i.e. the conductance decreases slightly with V_g, a feature already mentioned in some other systems (Be [9], GeSbTe [13], GeTe [14], GeBiTe [15]). It was suggested that the sign of this slope is controlled by the energy derivative of the thermodynamic density-of-states at the Fermi

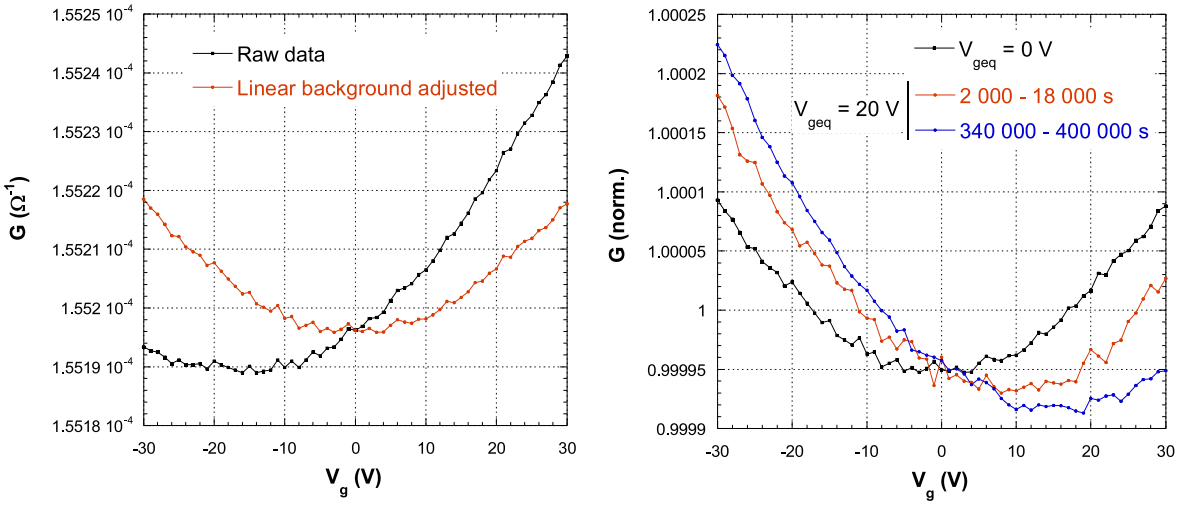

Figure 8. Left panel: $G(V_g)$ curve measured at room T after 20 days spent under $V_{geq} = 0\ V$. Black symbols: raw data; red symbols: linear background adjusted data. Right panel: evolution of the $G(V_g)$ curves (corrected for the linear background) when V_{geq} is changed from 0 V to 20 V. The $G(V_g)$ curves have been averaged over the time intervals indicated in the legend in order to improve the signal-to noise ratio. Amorphous $Nb_{13}Si_{87}$ film, 2.5 nm thick, $R_{s300K} = 25\ k\Omega$.

level [9]. Second, shortly after the film fabrication (typically a few hours), MDs are not seen. In the example of Fig. 9, a conductance minimum becomes clearly visible only after a few days at room T, when the resistance value has stabilised (in the example of Fig. 9, it reaches about 1 % between 0 V and 30 V). This last feature, which to our knowledge was not reported before, deserves further investigation. It may reflect a relationship between the resistance relaxation which follows the film fabrication and which is usually attributed to the evolution of Au grain shapes [25], and the MD formation. However, like in granular Al and amorphous NbSi films, V_{geq} changes lead to logarithmic-like relaxations of the conductance. The full MDs are clearly not visible in our V_g range, but since the curves are not strictly symmetrical, the actual MD width could not be estimated with precision. The amplitude of the MD observed between 0 V and 30 V grows from 0.3 % for $R_{s300K} = 30\ M\Omega$ to 1 % for $R_{s300K} = 15\ G\Omega$.

5. Room temperature electron glassiness in an amorphous InOx film

Insulating InOx is the archetypal electron glass system and its study at room T is thus of prime importance. But as we will now show, the identification of MDs and their relaxations turns out to be trickier than in the other systems. By using the same protocol as before, i.e. $G(V_g)$ curves are measured after a long enough stay under a given V_{geq} value (10 V in Fig. 10), no conductance minimum is visible even if we remove a linear field effect contribution. Instead, a fast increase of the conductance is observed around -20 V, i.e. the starting side of the V_g sweep, followed by a soft concave curvature

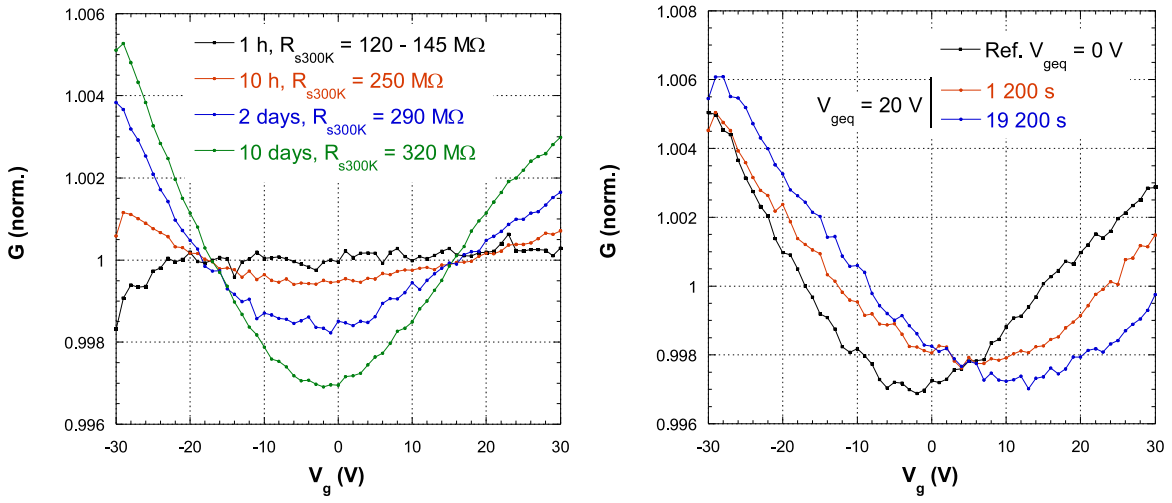

Figure 9. Left panel: evolution of the normalized $G(V_g)$ curves (corrected for a linear background) for a discontinuous Au film as a function of the time elapsed at room T since its fabrication. The R_{s300K} value also increases during this time. Right panel: $G(V_g)$ evolution resulting from a V_{geq} change from 0 V to 20 V.

at higher V_g values. The $G(V_g)$ curve can thus definitely not be interpreted as the mere sum of a linear normal field effect and a symmetrical MD centred on V_{geq}. Note also the large amplitude of the linear field effect contribution, which represents a 6 % change of G between 0 V and 20 V.

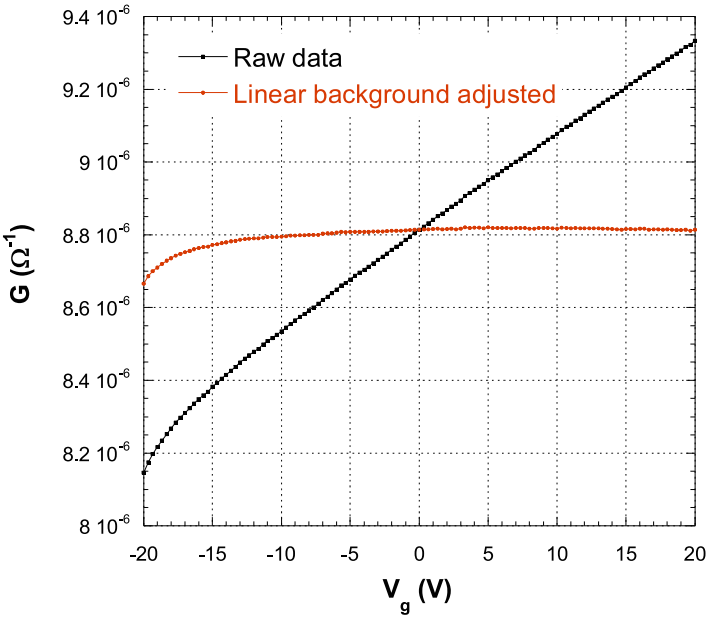

Figure 10. $G(V_g)$ curve measured at room T after 3 hours spent under $V_{geq} = 10\ V$. Black symbols: raw data; red symbols: linear background adjusted data (equalizing $G(0\ V)$ and $G(20\ V)$). Amorphous InOx film, $R_{s300K} \simeq 300\ k\Omega$.

If we now change V_{geq} from 10 V to -10 V, the time evolution of the normalized, linear background corrected curves is also quite startling (Fig. 11). Between sweep No 2 (curve S2, taken 1200 s after the change to -10 V) and the next ones, the normalized conductance is found to decrease continuously with time for negative V_g, and to increase for positive V_g (left panel of Fig. 11). A direct plot of the difference between sweep 2 and the following ones indeed suggests that the V_{geq} change provokes the formation of a wide MD centred on -10 V (right panel of Fig. 11). Its height between -10 V and 20 V amounts to 0.4 % of the conductance, which is larger than what we get in granular Al film having similar R_s values. Between sweep No 1 (curve S1, taken before the V_{geq} change) and sweep No 2 (curve S2), the conductance changes the opposite way, with an increase for negative V_g and a decrease for positive V_g.

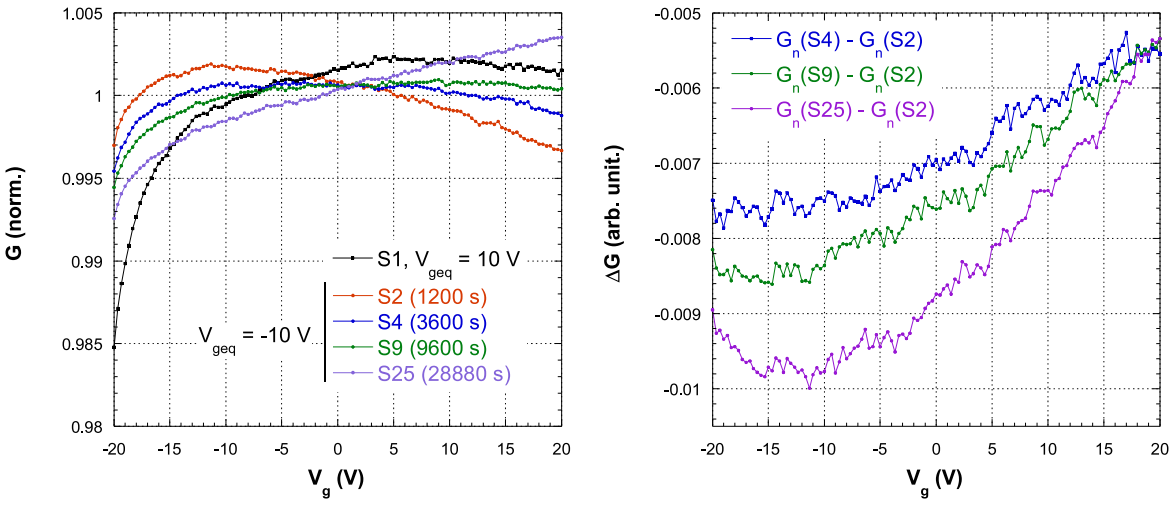

Figure 11. Left panel: time evolution of normalized $G(V_g)$ curves corrected for the linear background after V_{geq} is changed from 10 V to -10 V. Sn stands for "nth V_g sweep". S1 corresponds to the curve of Fig. 10, taken before the V_{geq} change. Right panel: differences between normalized $G(V_g)$ curves and S2 (vertically shifted in order to equalize their 20 V values). V_g sweeps are performed from left to right. Amorphous InOx film, $R_{s300K} \simeq 300\ k\Omega$.

One way to interpret this behaviour is to suppose that two sources of conductance relaxation are present: one which dominates the observed evolution between the two first scans S1 and S2, and the memory dip formation which dominates after the second scan S2. This hypothesis is supported by the following experiment. After a long stay under 0 V, we change the gate voltage to a new value and measure the time evolution of the conductance at that value (no V_g sweep). We compare what happens when V_g is switched from 0 to 20 V and from 0 to -20 V. If only the usual memory dip formation was present, the two relaxations would be roughly the same and consist in a slow $\ln(t)$ decrease of the conductance. However we observe two relaxations of opposite signs: a conductance increase if V_g is changed from 0 V to -20 V and a conductance decrease if it is changed from 0 V to 20 V. These are shown in Fig. 12a. It is seen that the

two conductance relaxations are not exactly opposite. By taking their half sum and difference, it is possible to isolate a dominant contribution which is anti-symmetrical with respect to the sign of the V_g jump, and a symmetrical one consisting of the usual downward logarithmic relaxation associated to the formation of a MD (see Fig. 12b and 12c). Note that the anti-symmetrical relaxation measured for 100 s is seven times larger than the one associated to the MD.

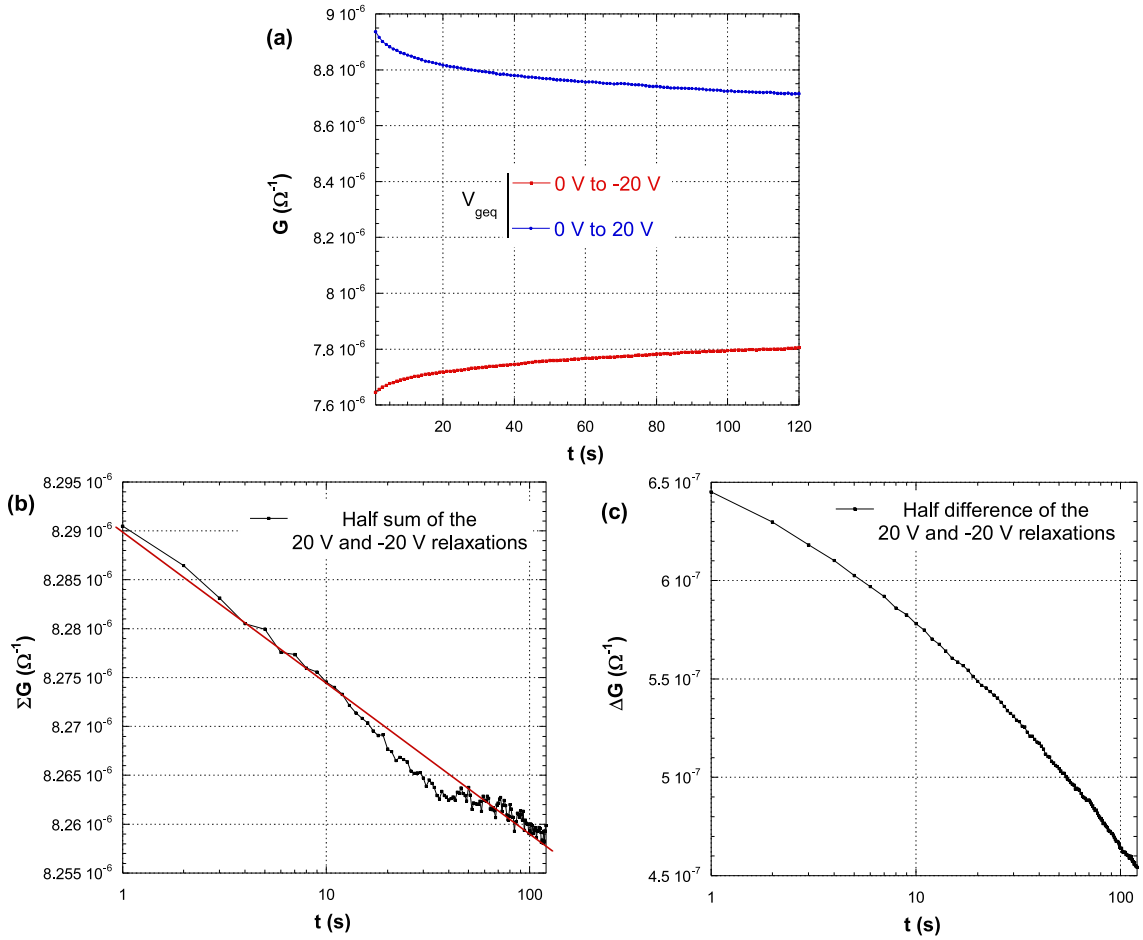

Figure 12. (a) Conductance relaxations measured after V_{geq} is changed from 0 to 20 V and from 0 to -20 V (see text for details). (b) Half sum of the 20 V and -20 V relaxations, corresponding to the "usual" MD formation (the red-line is a $\log(t)$ fit). (c) Half difference of the 20 V and -20 V relaxations, corresponding to an anti-symmetrical relaxation. Amorphous InOx film, $R_{s300K} \simeq 300\ k\Omega$.

The anti-symmetrical contribution explains qualitatively the anomalous S1 curve observed in Fig. 10. Just before sweep S1 started, V_g was changed from 10 V to -20 V. This -30 V jump caused an upward conductance drift during sweep S1, which mostly distorts the left part of the curve. Sweep S2 and the subsequent ones are preceded by a V_g jump three times smaller (from -10 V to -20 V). It gives rise to a smaller distortion of the curves, which can be eliminated by subtracting S2 from the subsequent curves. Hence the clear demonstration of the MD growth shown in Fig. 11 right panel.

We may be more quantitative and try to simulate the anti-symmetrical contribution to the curves of Fig. 10 and 11. In order to do so, we use the curve in Fig. 12c to represent the relaxation caused by a $\Delta V_g = 20\ V$ jump, and assume that for other jumps the relaxation is simply proportional to ΔV_g. The response for each V_g sweep is then simulated as the sum of the response to the initial negative V_g jump (start of the sweep, from V_{geq} to -20 V in that case) and to the successive small positive jumps composing the sweeps from -20 V to 20 V). Note that the conductance shift caused by the "normal" linear field effect is present in the response of Fig. 12c and is thus automatically taken into account in the simulation. An offset is added to make the simulated and actual curves coincide at $V_g = 20\ V$ (see Fig. 13-left). The difference between the measured and simulated conductance sweeps is expected to represent the MD relaxation contribution. As shown in Fig. 13-right, they indeed correspond to a MD around 10 V being progressively erased as a new one centred on -10 V is growing. The progressive shift to the left of the curves minimum is created by the strong overlap of the two MDs.

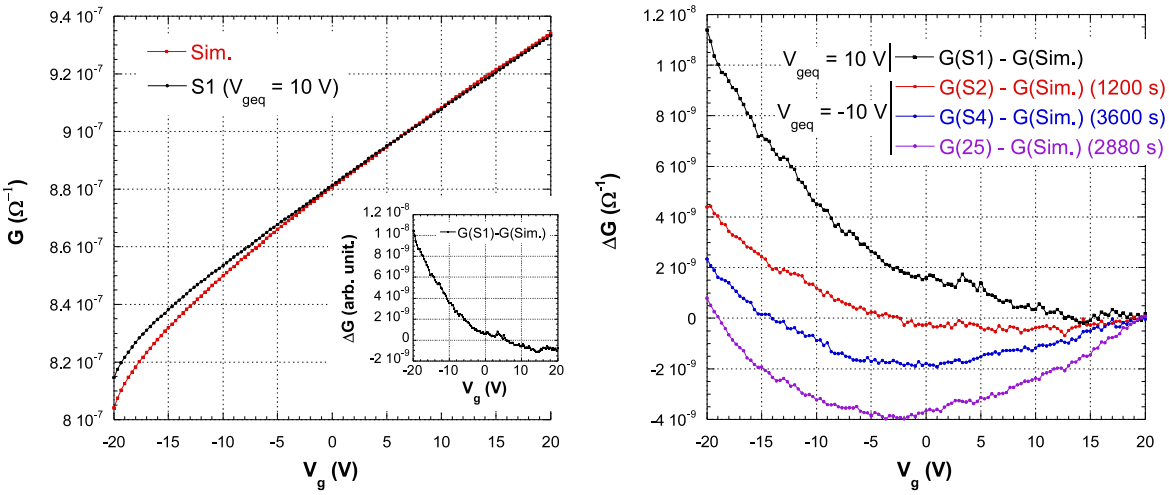

Figure 13. Left panel: $G(V_g)$ curve of Fig. 10 and 11 (S1) measured after 3 hours under $V_{geq} = 10\ V$ (black symbols). The simulated curve takes into account the anti-symmetrical relaxation (red symbols, see text for details). Insert: difference between the measured $G(V_g)$ curve (S1) and the simulated one. Right panel: time evolution of the difference between the measured $G(V_g)$ curves and the simulated ones after V_{geq} is changed from 10 V to -10 V. The progressive left shift of the curves minimum is created by the strong overlap of the fading 10 V MD and the growing -10 V one.

The precise origin of the anti-symmetrical relaxation is still unclear (no significant charging current is measured when the measurement of Fig. 12 is reproduced with a zero bias voltage). Interestingly enough, its relative amplitude decreases when T is lowered, which is contrary to the MD contribution. It thus becomes negligible compared to the latter at cryogenic temperatures. This T dependence suggests that the anti-symmetrical relaxation may be related to the movement of ionic species in the films, possibly oxygen

vacancies. Conductance relaxations induced by the drifts of oxygen vacancies under electric fields have been observed at room T in $SrTiO_3$ materials [30].

6. Why have room temperature glassy effects not been seen before?

Glassy effects are present in all the systems and all the samples we have been measuring: granular Al, amorphous NbSi, discontinuous Au and amorphous InOx film. We can thus legitimately ask why they were not highlighted much earlier? Instead, in InOx films studies, it has been constantly repeated that no memory dip can be measured above few tens of K [2, 3, 21, 31]. In the pioneer paper of 1991, it was written [2]: "At high T, regardless of R_s, the symmetrical component (the MD) does not appear. For example, a 1 $G\Omega$ amorphous film measured at 77 K did not exhibit any symmetrical component, while at low T, such R_s typically yield a 1 - 2 % effect (1 - 4 K)". This statement is in apparent contradiction with our findings. But according to the experimental results described previously, MDs are harder to identify at room T than at 4 K for at least three reasons. First, they are overlapped by a linear field effect which amplitude can be larger than the MDs themselves, especially for low R_s films. By comparison, the linear field effect remains relatively small at 4.2 K in granular Al films. Second, the MD amplitudes at room T in films usually measured in the liquid He range are small, typically less than 0.1 % in granular Al films (see Fig. 6). These amplitudes are found to grow with R_s and they reach values of the order of 1 % in granular Al films only when R_{s300K} lies above 1 $G\Omega$. The measurement of large MDs at room T thus requires the making of specific films, which due to the exponential-like divergence of the resistance at low T, can not be measured in the liquid He range. Third, the MDs at room T are very wide compared to what they are at 4.2 K. In order to see them, it is therefore absolutely necessary to measure $G(V_g)$ curves over a large enough V_g window. It was shown at 4.2 K that the MD dip width in a given sample is proportional to the thickness of the oxide layer used on the MOSFET device (it is the surface charge carrier density induced on the capacitor which matters [21, 34]). In our measurements, V_g can be safely swept between -30 V and 30 V over 100 nm of SiO_2 and only the bottom of the dips are visible in all the films investigated (the FHWMs lie above 100 V in our granular Al films). In previous InOx studies, much smaller values were used: $\pm 100\ V$ over 100 μm of glass [2, 3, 20, 35, 31] or $\pm 10\ V$ over 500 nm of SiO_2 [32, 33] respectively equivalent to $\pm 0.1\ V$ and $\pm 2\ V$ over 100 nm SiO_2. Such values do not allow the determination of MDs 100 V wide. In the granular Al film of Fig. 4 (right panel), a Lorentzian fit gives for the actual amplitude of the MD a relative value of 0.09 %. The amplitude falls to 0.02 % when measured between 0 and 30 V, to 10^{-4} % between 0 and 2 V and much below between 0 and 0.1 V, i.e. definitely below the noise level of the experiment. This problem is evident at room T, but might also be important at lower T. In the T study of InOx MD parameters published in Ref. [20], the MD plotted on Fig. 1 is clearly larger than the explored V_g range already at 4 K. An increase of the MD width with T, even if its actual amplitude is constant, will result in a decrease of its "apparent"

amplitude. If no fit of the data with some known functions is performed (Lorentzian, ...), it will not be possible to obtain a reliable temperature dependence for the MD amplitude. However, more recent T studies stress that the MD of some amorphous InOx films displays a very sharp decrease around 4 K, even for a T increase as small as 1 K [34]. In granular Al films, a similar T study was done over a larger V_g range with the use of Lorentzian fits for the $G(V_g)$ curves [8]. A softer power law dependence was obtained for the MD amplitude decrease with T.

A further point we would like to emphasize is the fact that long relaxation times are present in all the films and systems measured, whatever R_s and the MD amplitudes values. We found no evidence of some saturation to an equilibrium state, even after days of measurements, and thus no signs of a glass transition crossing between 4 K and room T. Instead, logarithmic time dependencies are observed, indicating that a wide distribution of relaxation times is still at work. The fact that the relaxation and MD relative amplitudes are smaller at room T than at lower T does not necessarily mean that the system is "faster" [36]. This smallness can indicate that less slow modes are present in the system, but also that the conductance is less sensitive to the slow modes. In the absence of a more precise and quantitative model, it is not possible to conclude.

7. Room temperature glassy effects and the electron glass hypothesis

Lastly, we would like to discuss whether the room T glassy effects reported here can be explained by the electron glass hypothesis.

Most of the numerical simulations on Coulomb glass models agree on the existence of a slowdown of the dynamics as T is lowered [37, 38, 39, 40, 41, 42, 1]. Such systems are characterized by a large number of metastable states, in which the transitions from one state to the other are believed to give rise, at low enough T, to relaxation times longer than any accessible experimental times [37, 38, 39]. The simultaneous hops of many electrons were found to play a crucial role in these very long relaxation times [37, 39, 42, 29, 43]. It was also suggested that the memory dip and its slow relaxation subsequent to V_{geq} changes are due to the slow rearrangement of many-electron clusters, which modify the occupation probability of the electronic sites participating to the transport [44, 29]. As to the existence of a true thermodynamic glass transition, the issue remains theoretically controversial. Mean field theories have predicted its existence in 3D and 2D systems [45, 46, 47]. T_g estimates were found to be strongly dependent on the system parameters, and possibly larger than the Coulomb gap energy in 2D systems having strong disorder and large charge carrier densities [48]. Numerical investigations found either no trace of such a transition [49], or T_g values much smaller than the mean field predictions [50].

A feature common to all these models is that electronic glassy effects manifest at temperatures smaller than the Coulomb gap energy U_{CG}, which is the typical energy scale below which electronic correlations become important. In a disordered system, U_{CG} is given in 3D by $\alpha e^3 (N(E_F))^{1/2} (4\pi\epsilon)^{-3/2}$, where $N(E_F)$ is the density of states at

the Fermi level, ϵ the effective dielectric constant and α a numerical constant close to unity [51]. In our InOx film, the MD width at 17 K (the lowest temperature at which the $G(V_g)$ curves were still measurable, $R = 17\ G\Omega$) is equal to $\simeq 4\ V$, which gives by extrapolation a MD width of $\simeq 1\ V$ at 4 K. By using the correlation between the charge carrier concentration n and the 4 K MD width reported in InOx films [32], we find that $n \approx 10^{20}\ e/cm^3$. Taking the free electron formula for $N(E_F)$ and a relative dielectric constant of 10 [2], we finally obtain $U_{CG} \approx 0.1\ eV$. In NbSi films, the charge carrier density is not known precisely but it may be larger than $10^{22} e/cm^3$ [12], which will correspond to a Coulomb gap charging energy above 0.2 eV (again assuming a relative dielectric constant of 10). In granular Al films, U_{CG} should be of the order of the charging energy of the Al grains. For a typical grain diameter of 5 nm and a tunnel barrier 1 nm-thick, we get a charging energy of the order of 100 K [8]. We should bear in mind that all these estimates have a high level of uncertainty: the relative dielectric constant is not precisely known in amorphous InOx and NbSi films, there is a distribution of grain size and tunnelling barriers in granular Al, and these parameters may change strongly at the approach of the metal-insulator transition. Energy distributions extending above 300 K thus seem plausible.

One may also consider activation energies extracted from transport and slow relaxation experiments. In insulating granular Al films the resistance diverges almost exponentially as T is lowered. Using it, we get a wide range of activation energies depending on the insulating character of the samples : from 1000 K when $R_{s300K} \approx 100\ G\Omega$ to 100 K when $R_{s300K} \approx 100\ k\Omega$. In granular Al films the MD dynamics was shown to depend on T in a complex manner, showing effective activation energies which depend on the temperatures involved in the measurements, and can be as high as 2000 K when the dynamics is measured around 50 K [52]. A similar behaviour was also recently observed in InOx [52].

However the picture is not that simple. First, the case of discontinuous Au is peculiar. This material presents a wide distribution of Au island size and shape (see Fig. 1) but many of them stretch on more than 100 nnm, which would imply charging energies of less than $\simeq 10\ K$. Activation energies estimates from resistance measurements are also smaller than in granular Al : for example less than 10 K when $R_{s300K} = 100\ M\Omega$. Second, according to a percolation approach of the memory effects, the MD width is expected to be proportional to $k_B T$ when the latter is larger than the coulomb gap [48]. Since this temperature dependence is approximately observed down to 4 K in granular Al, InOx and NbSi, one may deduce that U_{CG} is less than 1 meV !

Regardless of any specific model consideration, relaxation times as long as days ($\approx 10^5\ s$) at room T involve processes with activation energies as high as 0.5–1 eV (attempt rates between 10^{12} to $10^6\ s^{-1}$). In an intrinsic picture where these slow relaxations result from the rearrangement of electron clusters [44, 29], it implies either individual electron hops with activation energies of 0.5-1 eV, at the upper limit of our Coulomb gap energy estimates, or simultaneous hops of N electrons, each of it having a smaller average energy [44]. Whether such collective events are indeed present in

significant number at room T in our disordered films, especially not too far from the metal-insulator transition and in discontinuous Au films, deserves further theoretical and numerical studies.

8. Conclusion

We have identified for the first time electrical glassy features at room T in granular Al and InOx films. MDs are present in all the films we have been measuring. Their V_g-widths are about 100 times larger than what is usually found at 4 K, while their time evolutions under V_{geq} changes obey similar logarithmic dependences. The existence of room T glassy effects, so far only mentioned in discontinuous Au and NbSi films, seems to be the rule rather than the exception among electron glass systems.

Our study clarifies what experimental conditions are required in order to measure room T glassy effects. In particular, the large V_g widths of the MDs at room T require the use of a large enough V_g range in field effect measurement (or of a thin enough gate insulating material), a condition which was not fulfilled in previous attempts on InOx films. Some specific difficulties were also met: in discontinuous Au films, the MDs become measurable only a few hours after the making of the films, and in amorphous InOx films, the usual conductance relaxation is mixed with a relaxation mechanism of different nature. More extensive investigations are needed in order to clarify the physical origin of these two features.

The existence and the ability to measure electrical glassy effects up to room T open promising perspectives. First, it allows the use of new experimental techniques, such as local electrical probes, more difficult to implement in the liquid He range. Second, the knowledge of the MD evolution between 4 K and 300 K must help to build quantitative models of the electrical glassy effects and to precise the discrepancies/similarities between the different systems. In particular, a surprising T dependence was recently demonstrated for the glassy dynamics of granular Al and InOx films below 30 K [26, 52], with an increase of the apparent activation energy with T. It will be interesting to determine how the glassy dynamics evolves at higher T.

Acknowledgements

We acknowledge Claire Marrache-Kikuchi, Laurent Bergé and Louis Dumoulin for providing NbSi samples and for their comments on the article. We also gratefully acknowledge discussions with Markus Müller.

References

[1] Pollak M, Ortuño M and Frydman A 2012 *The Electron Glass* (Cambridge, UK: Cambridge University Press)
[2] Ben-Chorin M, Kowal D and Ovadyahu Z 1991 *Phys. Rev. B* **44** 3420
[3] Ben-Chorin M, Ovadyahu Z and Pollak M 1993 *Phys. Rev. B* **48** 15025

[4] Adkins C J, Benjamin J D, Thomas J M D, Gardner J W and McGeown A J 1984 *J. Phys. C: Solid State Phys.* **17** 4633
[5] Martinez-Arizala G, Grupp D E, Christiansen C, Mack A M, Markovic N, Seguchi Y and Goldman A M 1997 *Phys. Rev. Lett.* **78** 1130
[6] Havdala T, Eisenbach A and Frydman A 2012 *EPL* **98** 67006
[7] Grenet T 2003 *Eur. Phys. J. B* **32** 275
[8] Grenet T, Delahaye J, Sabra M and Gay F 2007 *Eur. Phys. J. B* **56** 183
[9] Ovadyahu Z, Xiong X M and Adams P W 2010 *Phys. Rev. B* **82** 195404
[10] Ovadyahu Z 2013 *Phys. Rev. B* **88** 085106
[11] Delahaye J, Grenet T, Marrache-Kikuchi C A, Drillien A A and Bergé L 2014 *EPL* **106** 67006
[12] Delahaye J, Grenet T, Marrache-Kikuchi C A, Humbert V, Bergé L and Dumoulin L 2020 *SciPost Phys.* **8** 56
[13] Ovadyahu Z 2015 *Phys. Rev. B* **91** 094204
[14] Ovadyahu Z 2016 *Phys. Rev. B* **94** 155151
[15] Ovadyahu Z 2018 *Phys. Rev. B* **97** 054202
[16] Davies J H, Lee P A and Rice T M 1982 *Phys. Rev. Lett.* **49** 758
[17] Grunewald M, Pohlmann B, Schweitzer L and Wurtz D 1982 *J. Phys. C: Solid State Phys.* **15** L1153
[18] Pollak M and Ortuño M 1982 *Solar Energy Materials* **8** 81
[19] Ovadyahu Z 2018 *Phys. Rev. B* **97** 214201
[20] Vaknin A, Ovadyahu Z and Pollak M 1998 *EPL* **42** 307
[21] Vaknin A, Ovadyahu Z and Pollak M 2002 *Phys. Rev. B* **65** 134208
[22] Eisenbach A, Havdala T, Delahaye J, Grenet T, Amir A and Frydman A 2016 *Phys. Rev. Lett.* **117** 116601
[23] Eisenbach A 2017 *Temperature-Dependent Dynamics in Disordered Metals*(Ph.D. thesis, Bar-Ilan University, Israel)
[24] Crauste O, Gentils A, Couëdo F, Dolgorouky Y, Bergé L, Collin S, Marrache-Kikuchi C A and Dumoulin L 2013 *Phys. Rev. B* **87** 144514
[25] Andersson T 1976 *J. of Appl. Phys.* **47** 1752
[26] Grenet T and Delahaye J 2017 *J. Phys.: Condensed Matter* **29** 455602
[27] Delahaye J, Honoré J and Grenet T 2011 *Phys. Rev. Lett.* **106** 186602
[28] Vaknin A, Ovadyahu Z and Pollak M 2000 *Phys. Rev. B* **61** 6692
[29] Amir A, Oreg Y and Imry Y 2011 *Ann. Rev. of Cond. Matter Phys.* **2** 235
[30] Delahaye J and Grenet T 2016 *J. Phys. D: Appl. Phys.* **49** 395303
[31] Ovadyahu Z 2006 *Phys. Rev. B* **73** 214204
[32] Vaknin A, Ovadyahu Z and Pollak M 1998 *Phys. Rev. Lett.* **81** 669
[33] Ovadyahu Z 2014 *Phys. Rev. B* **90** 054204
[34] Ovadyahu Z 2008 *Phys. Rev. B* **78** 195120
[35] Ovadyahu Z 2006 *Phys. Rev. B* **73** 214208
[36] Grenet T and Delahaye J 2012 *Phys. Rev. B* **85** 235114
[37] Pérez-Garrido A, Ortuño M, Díaz-Sánchez A and Cuevas E 1999 *Phys. Rev. B* **59** 5328
[38] Menashe D, Biham O, Laikhtman B D and Efros A L 2000 *EPL* **52** 94
[39] Tsigankov D N, Pazy E, Laikhtman B D and Efros A L 2003 *Phys. Rev. B* **68** 184205
[40] Grempel D R 2004 *EPL* **66** 854
[41] Somoza A M and Ortuño M 2005 *Phys. Rev. B* **72** 224202
[42] Bergli J, Somoza A M and Ortuño M 2012 *Phys. Rev. B* **85** 214202
[43] Ortuño M and Somoza A M 2012 *J. Phys.: Conf. Ser.* **376** 012007
[44] Kozub V I, Galperin Y M, Vinokur V and Burin A L 2008 *Phys. Rev. B* **78** 132201
[45] Müller M and Ioffe L B 2004 *Phys. Rev. Lett.* **93** 256403
[46] Pankov S and Dobrosavljević V 2005 *Phys. Rev. Lett.* **94** 046402
[47] Müller M and Pankov S 2007 *Phys. Rev. B* **75** 144201

[48] Lebanon E and Müller M 2005 *Phys. Rev. B* **72** 174202
[49] Goethe M and Palassini M 2009 *Phys. Rev. Lett.* **103** 045702
[50] Barzegar A, Andresen J, Schechter M and Katzgraber H G *Phys. Rev. B* **100** 104418
[51] Efros A L and Shklovskii 1975 *J. Phys. C: Solid State Phys.* **8** L49
[52] Grenet T 2018 *Non equilibrium dynamics in electron glasses: indications of a universal temperature dependence* (International workshop on The Superconductor-Insulator Transition and Low-Dimensional Superconductors, Villard-de-Lans, France) (2018).